Journal of Applied Polymer Science

# Transparent and Durable $SiO_2$-Containing Superhydrophobic Coatings on Glass

**Fang Li, Miao Du, Qiang Zheng**
Department of Polymer Science and Engineering, MOE Key Laboratory of Macromolecular Synthesis and Functionalization, Zhejiang University, Hangzhou 310027, China
Correspondence to: M. Du (E-mail: dumiao@zju.edu.cn) and Q. Zheng (E-mail: zhengqiang@zju.edu.cn)

**ABSTRACT:** We fabricated novel superhydrophobic coatings based on $SiO_2$ nanoparticles combined with $NH_2$-terminated silicone ($SN_2$) or $SN_2$-modified polyurethane ($SN_2$-prePU) by alternately spin-coating them onto glass slides. The final fabricated surface contained $SN_2/SiO_2$ or $SN_2$-prePU/$SiO_2$ bilayers. The conditions of spin-coating method were also explored. $SN_2$-prePU with different $SN_2$/prePU molar ratios were synthesized to study the influence of $SN_2$ ratio on the water contact angles of ultimate spin-coated surfaces. The surface was found to be tunable from hydrophobic to superhydrophobic by choosing $SN_2$-prePU with different $SN_2$/prePU molar ratios or $SN_2$ content. Water droplets easily rolled off on these superhydrophobic surfaces. Surfaces coated with $SN_2/SiO_2$ bilayers showed better transparency, whereas surfaces coated with $SN_2$-prePU(2 : 1)/$SiO_2$ bilayers exhibited better durability. Droplets of varied pH were prepared to test the anti-wettability of the coatings. Results showed that the as-coated surfaces had stable superhydrophobicity to droplets with pH values ranging from 1 to 14. © 2014 Wiley Periodicals, Inc. J. Appl. Polym. Sci. **2015**, *132*, 41500.

**KEYWORDS:** durable; spin-coating; superhydrophobic coating; transparent

Received 5 July 2014; accepted 8 September 2014
**DOI: 10.1002/app.41500**

## INTRODUCTION

Superhydrophobic surfaces can be potentially applied in self-cleaning,[1–3] anti-contamination,[4] anti-corrosion,[5] anti-fogging,[6] anti-sticking of snow,[7] and oil-water separation,[8] etc. Thus, studying and fabricating superhydrophobic surfaces has emerged as one of the most popular research topics in the past 15 years.[9,10] Superhydrophobic surfaces are those that display apparent water contact angles over 150°. Roughness and the surface free energy (or surface tension) are the two key factors that determine the hydrophobicity of surfaces.[11] During the past decade, intensive efforts have been exerted to develop new methods for preparing superhydrophobic surfaces that display micro- and nano-roughness. Various approaches involving physical and chemical methods have been used in constructing superhydrophobic surfaces. These approaches can be generally classified into top-down and bottom-up techniques, depending on the direction of the procedure. Top-down methods include lithographic etching,[12] template method,[13] methods which combine lithographic etching with template,[14] and plasma treatment,[15,16] etc. Bottom-up methods usually involve chemical deposition,[17–19] colloidal assembly,[20,21] layer-by-layer assembly,[22,23] hydrogen bond-based methods,[24] and phase separation-based methods,[25] etc. There are also some methods which combine top-down and bottom-up methods, like coating polymer solutions[26,27] or polymer-inorganic nanoparticle solutions,[28,29] etc. Top-down approaches can fabricate excellent micro- and nano-structures with controllable sizes, shapes, morphology, and topography. However, these approaches are comparatively complex and not feasible for large-area fabrication.[30] On the other hand, bottom-up methods are cost effective and have potential application in the fabrication of large-area superhydrophobic surfaces. Among them, spin-coating is a facile but effective method, by which the roughness and the anti-wettability can be tuned.[31,32]

For applications, several limitations need to be solved, such as transparency, durability, ability of retaining superhydrophobicity under different pH, and ability of shielding inner surfaces from corrosive liquids, etc. Various studies have attempted to fabricate transparent superhydrophobic surfaces.[33,34] However, these surfaces either lack fine durability or need further durability tests. A good balance between transparency and durability still remains unsolved. On one hand, to obtain a transparent superhydrophobic surface, the micro- and nano-structures should be precisely tuned given that transparency and superhydrophobicity have two paradoxical requirements for the hierarchical structure. On the other hand, although the study on durability is

Additional Supporting Information may be found in the online version of this article.

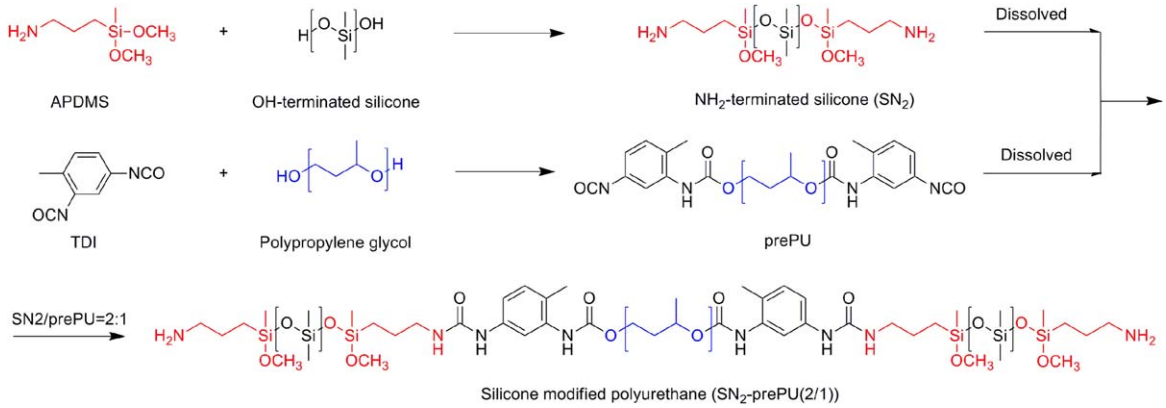


**Scheme 1.** Preparation of $SN_2$ and $SN_2$-prePU. [Color figure can be viewed in the online issue, which is available at wileyonlinelibrary.com.]

quite important, only a few studies have focused on this characteristic.[35,36] Even less have succeeded in fabricating surfaces, which show superhydrophobicity to acidic or alkaline liquids.[37]

In this article, we will introduce a facile way to fabricate superhydrophobic surfaces by spin-coating $SiO_2$ nanoparticles and $NH_2$-terminated silicone (denoted as $SN_2$) or $SN_2$-modified polyurethane (denoted as $SN_2$-prePU) with nontoxic solvent. The anti-wettability, transparency, and durability of these surfaces were investigated. Aqueous solutions with pH values from 1 to 14 were prepared to inspect the anti-wettability of the as-coated surfaces under acidic and alkaline conditions.

## EXPERIMENTAL

### Materials

Polypropylene glycol (PPG, $M_w = 1000$ g/mol) was purchased from Gaoqiao Petrochemical Co., Ltd., Shanghai, China and was vacuum distilled to dehydrate. Hydroxyl-terminated poly(dimethyl siloxane) (OH-terminated PDMS, hydroxyl value is 4 wt %) was purchased from Quanli Chemical Co., Ltd., Wuxi, China. Amino propyl dimethoxymethyl silane (APDMS) was purchased from Debang Chemical New Materials Co., Ltd., Hubei, China. Toluene diisocyanate (TDI) was purchased from Tokyo Chemical Industry Co., Ltd., Japan. Tetraethyl orthosilicate (TEOS), ethanol and isopropanol were purchased from Sinopharm Chemical Reagent Co., Ltd., China. Ammonia was purchased from Hangzhou Changzheng Chemical Reagent Co., Ltd., China. All reagents were used without further purification. Ultrapurified water (UP-water) was laboratory-made.

### Preparation of $SiO_2$ Nanoparticles

$SiO_2$ nanoparticles were prepared through Stöber sol-gel method.[38,39] 40 mL TEOS was diluted with 600 mL ethanol and 100 mL UP-water in a flask. The solution were stirred for 15 min. Then, 7 mL ammonia was added into the flask while under strong stirring. Stirring was continued for 24 h at 35°C. The number-average diameter of the particle was around 100 nm, which was measured by dynamic light scattering.

### Preparation of $SN_2$ and $SN_2$-PrePU

Scheme 1 shows the fundamental synthetic route of $SN_2$ and $SN_2$-prePU. The top equation in Scheme 1 shows the synthesis of $SN_2$ (S represents silicone; $N_2$ represents two $NH_2$ functional end groups in the molecule). APDMS (2 mol) and OH-terminated PDMS (1 mol) were added into the flask, under moderate stirring at 110–120°C. The by-product methanol was vacuum distilled. The reaction was kept for 3 to 4 h until no methanol was produced.[40]

To synthesize $SN_2$-prePU, prePU was first synthesized with a fixed amount of PPG and TDI [The middle equation in Scheme 1]. The theoretical NCO amount was set at 5% and the final actual value of NCO amount was measured by titration to ensure that the reaction finished. Then, the quantified prePU and $SN_2$ were dissolved in isopropanol, respectively. The prePU solution was added dropwise into the $SN_2$ solution, and the mixture was stirred for another 30 min.

$SN_2$/prePU with various ratios were synthesized by programs displayed in Scheme 1. $SN_2$-prePU($x$ : $y$) is the abbreviation of $SN_2$-modified polyurethane with a certain $SN_2$/prePU ratio ($x$ is the molar of $SN_2$ and $y$ is the molar of prePU). A sample information is listed in Table II.

Figure 1 shows the FTIR spectrum of the synthesized $SN_2$-prePU(2 : 1) as a typical example of a series of $SN_2$-prePU with different ratios. The peak at 3311 $cm^{-1}$ can be attributed to the N—H stretching vibration. The peaks at 2962 and 2898 $cm^{-1}$

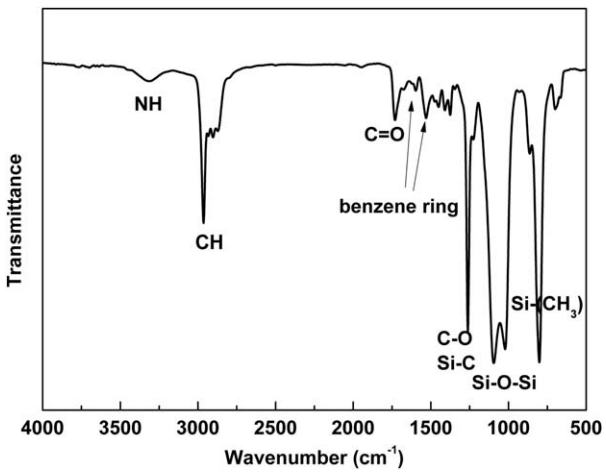


**Figure 1.** FTIR spectrum of the synthesized $SN_2$-prePU(2 : 1).

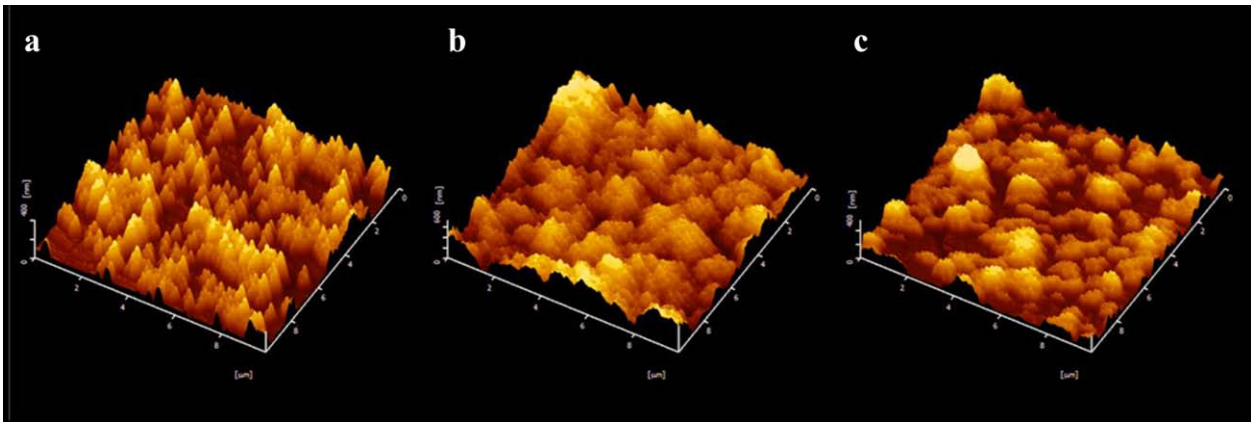


**Figure 2.** AFM 3D graphs of (a) surface *a*, 5 spin-coated $SiO_2$ layers, (b) surface *b*, 5 spin-coated $SN_2/SiO_2$ bilayers, and (c) surface *c*, 5 of spin-coated $SN_2$-prePU(2 : 1)/$SiO_2$ bilayers. [Color figure can be viewed in the online issue, which is available at wileyonlinelibrary.com.]

represent the C—H stretching vibration of $CH_3$, whereas the peaks at 2946 and 2863 $cm^{-1}$ correspond to the C—H stretching vibration of $CH_2$. The peak at 1730 $cm^{-1}$ can be attributed to the C=O stretching vibration of the urea and urethane groups. The peaks at 1694 and 1527 $cm^{-1}$ are the characteristic peak for benzene ring of TDI. The peak at 1261 $cm^{-1}$ corresponds to the stretching vibration of C—O and Si—C. The peaks at 1095 and 1022 $cm^{-1}$ are attributed to Si—O—Si stretching vibration. All characteristic peaks can be found on the FTIR spectra of other $SN_2$-prePU. The only difference of these FTIR spectra is the peak intensity of these characteristic peaks, which is due to the different $SN_2$/prePU ratios of $SN_2$-prePU. The calculated molecular weight of $SN_2$/prePU(2 : 1) is 3897 g/mol. The molecular weight measured by gel permeation chromatography is 3804 g/mol. These results indicate that $SN_2$/prePU(2 : 1) is synthesized as designed.

### Spin-Coat Superhydrophobic Surfaces

The $SN_2$ solution (or $SN_2$-prePU solution) and $SiO_2$ dispersion were diluted in nontoxic solvents, such as ethanol or isopropanol. The concentration of $SN_2$ or $SN_2$-prePU solution was 0.25 wt %, whereas the concentration of $SiO_2$ was 1.0 wt %. For the surface fabricated by $SN_2/SiO_2$ bilayers, the $SN_2$ solution was first spin-coated onto a glass slide at 3000 rpm. Second, the $SiO_2$ dispersion was spin-coated onto the afore-coated glass. These procedures were repeated for desired times and then the surface has several $SN_2/SiO_2$ bilayers. At last, the $SN_2$ solution was spin-coated on the topside. For the surface coated with $SN_2$-prePU/$SiO_2$ bilayers, only the organic component $SN_2$ was replaced by $SN_2$-prePU, and the other procedures were the same.

### Characterization

Contact angles were measured by an optical contact angle measuring device (Harke-SPCA, Peking Harke Experimental Instrument Factory, China). The transmittance of the surfaces was characterized using UV–vis spectrophotometer (CARY 100 Bio, Varian Inc., USA). The transmittance data ($T$%) plotted in Figure 5(b) is calculated using the formula, $T\% = \frac{T_c}{T_{glass}} \times 100\%$, where $T_c$ is the transmittance of coated surfaces and $T_{glass}$ is the transmittance of the untreated glass slide. The morphology was observed using the atomic force microscope (AFM, in DFM mode, SPI3800N, SII Nano Technology Inc., Japan). The arithmetical mean deviation of the surface, $R_a = \frac{1}{n}\sum_{i=1}^{n}|y_i|$ ($y_i$ is the vertical distance from the mean line to the $i$th data point in the scan region), the root mean square of surface, $RMS = \sqrt{\frac{1}{n}\sum_{i=1}^{n} y_i^2}$, the maximum height of the surface profile, P-V = $R_p$-$R_v$ (in which $R_p = \max_i y_i$. $R_v = \min_i y_i$), and the quotient of the exact surface area to the project area, $S$ Ratio, can be measured using AFM.

## RESULTS AND DISCUSSION

### Static Water Contact Angle

Spin-coating could lead to close-packed colloidal crystals because of shear-induced ordering.[41,42] It is also positive to have the close-pack of $SiO_2$ nanoparticles, since aggregation enlarges the surface roughness, which further generates the superhydrophobicity of the surface according to Wenzel model or Cassie-Baxter model.[43,44] However, the interaction between rigid $SiO_2$ and $SiO_2$ nanoparticles is not large enough to guarantee a stable surface structure. As a result, the supernormal anti-wettability wrecks in a short time. Thus, $SN_2$ and $SN_2$-prePU are introduced. And the morphology of the surfaces spin-coated with different compositions were studied. The surface coated with 5 $SiO_2$ layers is denoted as surface *a*; the surface coated with 5 $SN_2/SiO_2$ bilayers is denoted as surface *b*; and the surface coated with 5 $SN_2$-prePU(2 : 1)/$SiO_2$ bilayers is denoted as surface *c*. The surface morphology is investigated using AFM and Figure 2 shows 3D topographic graphs of these surfaces. The surface information are listed in Table I. The light and rough area in Figure 2(a–c) indicates the surfaces that were covered with $SiO_2$.

**Table I.** Surface Information of Surface *a*, Surface *b*, and Surface *c*

| Surface | $R_a$ (nm) | RMS (nm) | P-V (nm) | S ratio | $\theta_w$ (°) |
|---|---|---|---|---|---|
| a | 72.3 | 83.8 | 400.9 | 1.198 | 45.3 ± 5.2 |
| b | 100.5 | 125.9 | 723.7 | 1.272 | 128.8 ± 3.1 |
| c | 68.1 | 83.3 | 547.1 | 1.230 | 124.5 ± 3.9 |

**Note:** surface a, 5 spin-coated $SiO_2$ layers; surface b, 5 spin-coated $SN_2/SiO_2$ bilayers; surface c, 5 spin-coated $SN_2$-prePU(2 : 1)/$SiO_2$ bilayers.

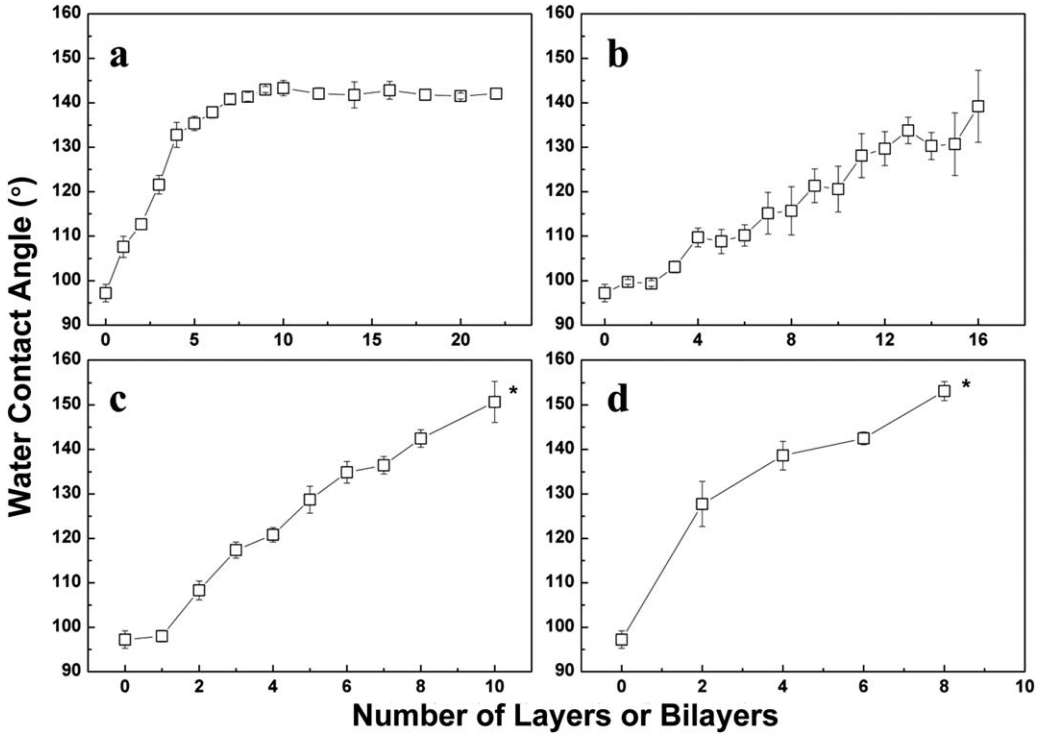


**Figure 3.** (a) $\theta_w$ of surfaces spin-coated with only $SiO_2$ layers at 2000 rpm. (b) $\theta_w$ of surfaces spin-coated with $SN_2/SiO_2$ bilayers at 2000 rpm, while the solvent is isopropanol. (c) $\theta_w$ of surfaces spin-coated with $SN_2/SiO_2$ bilayers at 2000 rpm. (d) $\theta_w$ of surfaces spin-coated with $SN_2/SiO_2$ bilayers at 3000 rpm. If it is not specially pointed out, the solvent is ethanol.

The $SiO_2$ coverage of surface *b* is much higher than those from surfaces *a* and *c*. Meanwhile, the $R_a$, RMS, P-V, and S Ratio of surface *b* are also larger than those from the other two, implying a rougher surface structure. These results indicate that $SN_2$ can help $SiO_2$ with the formation of a rougher surface structure to some extent. Thus, surface *b* exhibits the largest water contact angle ($\theta_w$). Surface *a* has a similar $R_a$ and RMS to those of surface *c*. However, the $\theta_w$ of surface *c* is much larger than that of surface *a*, which demonstrates that the organic component ($SN_2$ in $SN_2$-prePU) endows the surface with low surface energy and improves the anti-wettability of the spin-coated surface.

The conditions of the spin-coating method like rotational speed and solvent influence the morphology and will finally affect the hydrophobicity of the surfaces. Thus, the $\theta_w$ of the surfaces spin-coated with $SiO_2$ alone or $SN_2/SiO_2$ under different conditions were measured and displayed in Figure 3(a–d). It should be specifically pointed out that the glass slides were all coated with one layer of $SN_2$ first to enable all the surfaces at the same original spin-coating condition. Hence, the surface spin-coated with once $SN_2$ layer is denoted as the surface spin-coated with 0 bilayer or $SiO_2$ mono layer and the corresponding $\theta_w$ is $97.2 \pm 2.0°$. For surfaces spin-coated with only $SiO_2$, the horizontal ordinate represents the layers of $SiO_2$. For other spin-coated surfaces, the horizontal ordinate represents the bilayers. The increase in layers or bilayers results in the increase in $\theta_w$ for all surfaces, which is believed that the increasing layers or bilayers enlarges the roughness of the surface structure as well as the hydrophobicity. However, in Figure 3(a), as the spin-coated time exceeds 10, the $\theta_w$ of the surfaces coated with $SiO_2$ layers displays around 140°, showing no further increment. However, the $\theta_w$ of the surfaces coated with $SN_2/SiO_2$ bilayers increase monotonously with the number of spin-coated bilayers [Figure 3(b–d)].

The solvent also plays an important role in constructing rough surfaces. The surfaces obtained using ethanol as the solvent showed larger $\theta_w$ than those obtained using isopropanol as can be seen by comparing Figure 3(b) with Figure 3(c). Because of the weaker polarity of isopropanol than ethanol, it is more compatible with both organic and inorganic components.[45] Also, isopropanol volatilizes slower than ethanol during spin-coating, which offers the components much more time to disperse homogeneously on the surface. Consequently, isopropanol facilitates the formation of a smoother surface structure, which generates lower $\theta_w$. In addition, a higher rotational speed favors the dispersion of $SiO_2$ particles.[41] Thus, the surfaces spin-coated at 3000 rpm [Figure 3(d)] exhibit larger $\theta_w$ than the surface spin-coated at 2000 rpm [Figure 3(c)] under the same spin-coated times. The symbol "*" in Figure 3(c,d) indicates that a sessile droplet test cannot proceed on coated surfaces with more bilayers because the superhydrophobicity of the surfaces prevents water droplet adhesion. Water droplets can roll off easily on these superhydrophobic surfaces when they are slightly tilted (Supporting Information Video S1). When water is injected onto them, water droplets bounce off the surfaces at once (Supporting Information Video S2, some areas of the glass are not coated with the superhydrophobic coatings to illustrate the difference more clearly).

**Table II.** Composition Information of $SN_2$ and Selected $SN_2$-prePU and $\theta_w$ of the Surfaces Spin-Coated with 20 $SN_2/SiO_2$ Bilayers or 20 $SN_2$-prePU/$SiO_2$ Bilayers.

| Sample abbreviation | $SN_2$ (mol) | prePU (mol) | $\theta_w$ (°) |
|---|---|---|---|
| $SN_2$ | 1 | / | >160 |
| $SN_2$-prePU(1 : 1.4) | 1 | 1.4 | 133.2 ± 1.6 |
| $SN_2$-prePU(1.4 : 1) | 1.4 | 1 | 140.1 ± 0.3 |
| $SN_2$-prePU(1.6 : 1) | 1.6 | 1 | 154.9 ± 1.1 |
| $SN_2$-prePU(1.8 : 1) | 1.8 | 1 | 153.4 ± 2.6 |
| $SN_2$-prePU(2 : 1) | 2 | 1 | 159.2 ± 1.4 |

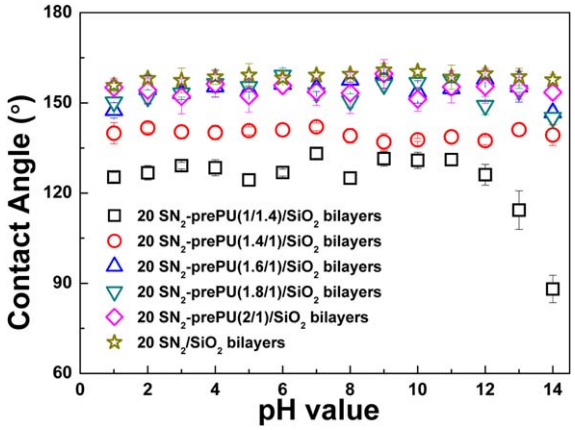


**Figure 4.** Contact angles for droplets of different pH on spin-coated surfaces. [Color figure can be viewed in the online issue, which is available at wileyonlinelibrary.com.]

Using the optimized conditions (solvent: ethanol; rotational speed: 3000 rpm), both $SN_2/SiO_2$ bilayers and $SN_2$-prePU/$SiO_2$ bilayers are spin-coated onto the glass slides. For comparison, the number of spin-coated bilayers for these surfaces is set to be 20. Table II shows the water contact angles of surfaces spin-coated with different organic components, that is, $SN_2$ or $SN_2$-prePU with different compositions. The $\theta_w$ was observed to increase with increasing of $SN_2$ molar ratio in the $SN_2$-prePU. When the molar ratio of $SN_2$/prePU is higher than 1.6 : 1, the coated surfaces become superhydrophobic ($\theta_w > 150°$). The $R_a$ and RMS surface spin-coated with 20 $SN_2/SiO_2$ bilayers are 498.0 and 594.0 nm, respectively, whereas the $R_a$ and RMS of the surface spin-coated with 20 $SN_2$-prePU(2 : 1)/$SiO_2$ bilayers are 121.3 and 154.6 nm, respectively. The data in Table I further supports the idea that $SN_2$ helps in the formation of a rougher structure than $SN_2$-prePU while the number of bilayers are equal. Therefore, $SN_2$ not only decreases the surface energy of the coated surface but also favors a much rougher structure. The decrease in surface energy and the increase in surface roughness will be beneficial for the fabrication of superhydrophobic surfaces. Hence, the surface coated with more $SN_2$ displays better anti-wettability, and thus, showing greater $\theta_w$.

### Contact Angle to Droplets of Varied pH

Stable superhydrophobicity under varied pH conditions can expand the possible application of the superhydrophobic surfaces and can also shield the coated substrates from corrosive liquids, lengthening their service time. Figure 4 shows that except for the surface coated with 20 $SN_2$-prePU(1 : 1.4)/$SiO_2$ bilayers, all the spin-coated surfaces show stable contact angles to droplets of different pH, which indicates the stable anti-wettability. Specifically, the surfaces coated with 20 $SN_2$-prePU(1.6 : 1)/$SiO_2$ bilayers, 20 $SN_2$-prePU(1.8 : 1)/$SiO_2$ bilayers, 20 $SN_2$-prePU(2 : 1)/$SiO_2$ bilayers, and 20 $SN_2/SiO_2$ bilayers show contact angles larger than 150° to the droplets of pH ranging from 1 to 14. In other words, the superhydrophobic surfaces we fabricated were able to exhibit stable antiwettability under either acidic or alkaline conditions.

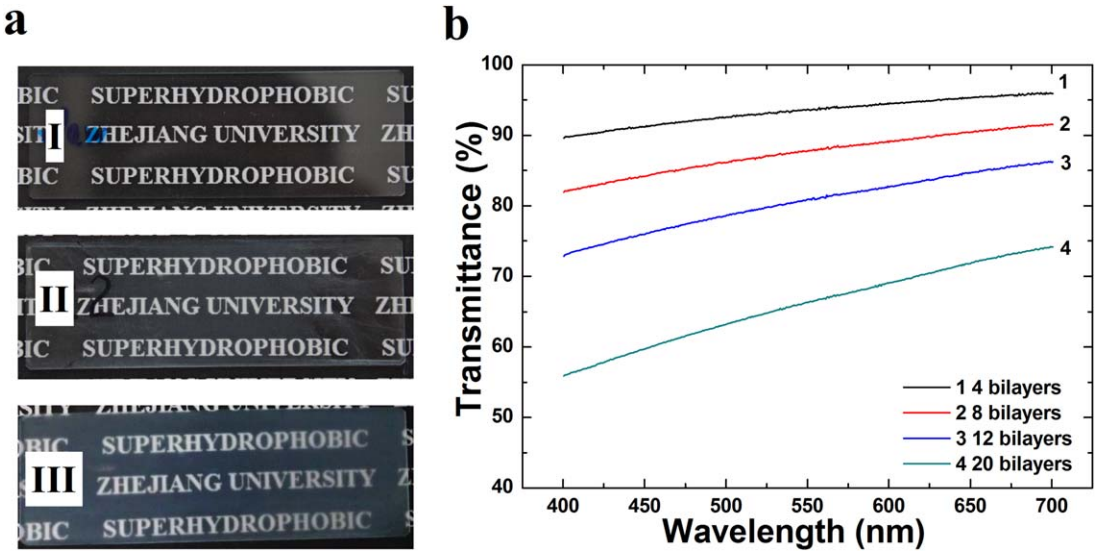


**Figure 5.** (a) Photographs for (I) untreated glass slide, (II) the glass slide coated with 20 $SN_2/SiO_2$ bilayers and (III) the glass slide coated with 20 $SN_2$-prePU(2 : 1)/$SiO_2$ bilayers. (b) Transmittance of surfaces spin-coated with different $SN_2/SiO_2$ bilayers. [Color figure can be viewed in the online issue, which is available at wileyonlinelibrary.com.]

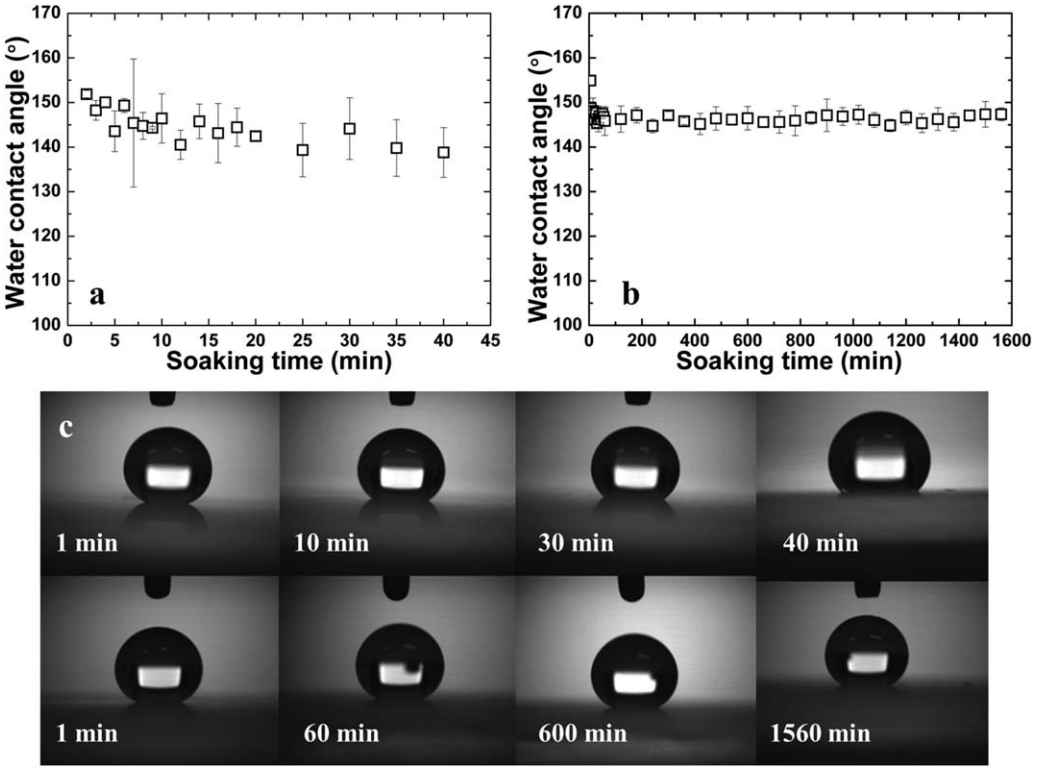


**Figure 6.** $\theta_w$ of the surfaces spin-coated with (a) 20 $SN_2/SiO_2$ bilayers and (b) 20 $SN_2$-prePU(2 : 1)/$SiO_2$ bilayers for different soaking time. (c) Photographs of water droplets on the spin-coated surfaces at different soaking time points. The upper four photographs are for the superhydrophobic surface coated with 20 $SN_2/SiO_2$ bilayers and the lower four photographs are for the superhydrophobic surface coated with 20 $SN_2$-prePU(2 : 1)/$SiO_2$ bilayers.

### Transparency of Spin-Coated Surfaces

Figure 5(a) shows the contrast of transparency between the untreated glass slide (I), the glass slide spin-coated with 20 $SN_2/SiO_2$ bilayers (II), and the glass slide spin-coated with 20 $SN_2$-prePU(2 : 1)/$SiO_2$ bilayers (III). The surface coated with 20 $SN_2/SiO_2$ bilayers (II) exhibited good transparency. Compared with the surface coated with 20 $SN_2/SiO_2$ bilayers (II), the surface coated with 20 $SN_2$-prePU(2 : 1)/$SiO_2$ bilayers (III) shows slight opacity, which could be attributed to the micro-phase separation between $SN_2$ and PU blocks. Figure 5(b) shows the transmittance of the as-fabricated surfaces with different $SN_2/SiO_2$ bilayers. The transmittance decreases with the increase in the number of bilayers. The transmittance of the surfaces spin-coated with 8 and 12 $SN_2/SiO_2$ bilayers still remains at a high level. The surface coated with eight bilayers exhibits not only superhydrophobicity [Figure 3(d)], but also good transparency (transmittance $>$ 80% in wavelength ranging from 400 to 700 nm).

### Durability of the Spin-Coated Surfaces

Durability is important in the long-time application of superhydrophobic surfaces. The glass slides spin-coated with 20 $SN_2/SiO_2$ bilayers and 20 $SN_2$-prePU(2 : 1)/$SiO_2$ bilayers were soaked into water and were taken out from the water for 1 min. Afterwards, the $\theta_w$ was measured, and the coated glass slides were soaked in water for another 1 min. Figure 6(a,b) show the $\theta_w$ of the superhydrophobic surfaces coated with 20 $SN_2/SiO_2$ bilayers and 20 $SN_2$-prePU(2 : 1)/$SiO_2$ bilayers, respectively, after different soaking times. For the surface coated with 20 $SN_2/SiO_2$ bilayers, the $\theta_w$ of some parts falls immediately to lower than 150° just after being soaked for 2 min. The coatings are further damaged by water after being soaked for another 4 min, displaying a further decrement of $\theta_w$, which can be down to approximate 130° on some areas of the coating and a much larger standard deviation. After being soaked for 40 min, most areas of the coated surface show irreversible damage. The huge $\theta_w$ decrement can be distinctly observed from the droplet shapes at different time points in the upper four photographs in Figure 6(c). Due to the low adhesive strength of $SN_2$ onto glass slides, the surface coated with 20 $SN_2/SiO_2$ bilayers can only retain its superhydrophobicity for several minutes when it is soaked into water.

The surface coated with $SN_2$-prePU(2 : 1)/$SiO_2$ bilayers, however, can retain its superhydrophobicity (stable $\theta_w$ around 150°) when it has been soaked into water for 26 h, despite the occurrence of a little decrement at the very beginning of the test. The droplet retains its spherical shape after being soaked for different times [lower four photographs in Figure 6(c)]. The existence of PU components enhances the adhesive strength within $SN_2$-prePU(2 : 1)/$SiO_2$ bilayers and between the coatings and the glass slide, avoiding the damage of the coatings. As a result, the durability of the coating increases.

## CONCLUSIONS

Superhydrophobic coatings made with cheap and easy-synthesized materials ($SN_2$ or $SN_2$-prePU as the organic

component and $SiO_2$ nanoparticles as the inorganic component) were fabricated by a convenient spin-coating method. Increasing the number of $SN_2/SiO_2$ bilayers or $SN_2$-prePU/$SiO_2$ bilayers and increasing the $SN_2$ molar ratio in the organic component $SN_2$-prePU of the coatings are beneficial for the hydrophobicity of the as-obtained surfaces. The largest water contact angle can be larger than 160°, and the water droplets can easily rolled off the superhydrophobic surfaces. The surface coated with $SN_2/SiO_2$ shows good transparency, whereas the surface coated with $SN_2$-prePU(2 : 1)/$SiO_2$ exhibits excellent durability. Both superhydrophobic surfaces coated with $SN_2/SiO_2$ bilayers and $SN_2$-prePU/$SiO_2$ bilayers exhibit stable super antiwettability to droplets of varied pH values ranging from 1 to 14.

## ACKNOWLEDGMENTS

This work was supported by the National Natural Science Foundation of China (Key Program, Grant 51333004) and the Program for Zhejiang Provincial Innovative Research Team (Grant No. 2011R09004-15).

## REFERENCES

1. Parkin, I. P.; Palgrave, R. G. *J. Mater. Chem.* **2005**, *15*, 1689.
2. Furstner, R.; Barthlott, W.; Neinhuis, C.; Walzel, P. *Langmuir* **2005**, *21*, 956.
3. Otten, A.; Herminghaus, S. *Langmuir* **2004**, *20*, 2405.
4. Lafuma, A.; Quere, D. *Nat. Mater.* **2003**, *2*, 457.
5. Liu, K.; Jiang, L. *Nanoscale* **2011**, *3*, 825.
6. Chiou, N.-R.; Lui, C.; Guan, J.; Lee, L. J.; Epstein, A. *J. Nat. Nanotechnol.* **2007**, *2*, 354.
7. Tarwal, N. L.; Patil, P. S. *Appl. Surf. Sci.* **2010**, *256*, 7451.
8. Feng, L.; Zhang, Z.; Mai, Z.; Ma, Y.; Liu, B.; Jiang, L.; Zhu, D. *Angew. Chem. Int. Ed.* **2004**, *43*, 2012.
9. Erbil, H. Y.; Demirel, A. L.; Avci, Y.; Mert, O. *Science* **2003**, *299*, 1377.
10. Xie, Q. D.; Fan, G. Q.; Zhao, N.; Guo, X. L.; Xu, J.; Dong, J. Y.; Zhang, L. Y.; Zhang, Y. J.; Han, C. C. *Adv. Mater.* **2004**, *16*, 1830.
11. Li, X.-M.; Reinhoudt, D.; Crego-Calama, M. *Chem. Soc. Rev.* **2007**, *36*, 1350.
12. Shiu, J. Y.; Kuo, C. W.; Chen, P. L.; Mou, C. Y. *Chem. Mater.* **2004**, *16*, 561.
13. Jin, M.; Feng, X.; Feng, L.; Sun, T.; Zhai, J.; Li, T.; Jiang, L. *Adv. Mater.* **2005**, *17*, 1977.
14. Li, J.; Fu, J.; Cong, Y.; Wu, Y.; Xue, L.; Han, Y. *Appl. Surf. Sci.* **2006**, *252*, 2229.
15. Ruiz, A.; Valsesia, A.; Ceccone, G.; Gilliland, D.; Colpo, P.; Rossi, F. *Langmuir* **2007**, *23*, 12984.
16. Kim, S. H.; Kim, J. H.; Kang, B. K.; Uhm, H. S. *Langmuir* **2005**, *21*, 12213.
17. Zhao, N.; Shi, F.; Wang, Z. Q.; Zhang, X. *Langmuir* **2005**, *21*, 4713.
18. Ma, M. L.; Mao, Y.; Gupta, M.; Gleason, K. K.; Rutledge, G. C. *Macromolecules* **2005**, *38*, 9742.
19. Hosono, E.; Fujihara, S.; Honma, I.; Zhou, H. S. *J. Am. Chem. Soc.* **2005**, *127*, 13458.
20. Hikita, M.; Tanaka, K.; Nakamura, T.; Kajiyama, T.; Takahara, A. *Langmuir* **2005**, *21*, 7299.
21. Zhang, G.; Wang, D. Y.; Gu, Z. Z.; Mohwald, H. *Langmuir* **2005**, *21*, 9143.
22. Han, J. T.; Zheng, Y.; Cho, J. H.; Xu, X.; Cho, K. *J. Phys. Chem. B* **2005**, *109*, 20773.
23. Shi, F.; Wang, Z.; Zhang, X. *Adv. Mater.* **2005**, *17*, 1005.
24. Han, J. T.; Lee, D. H.; Ryu, C. Y.; Cho, K. W. *J. Am. Chem. Soc.* **2004**, *126*, 4796.
25. Jiang, L.; Zhao, Y.; Zhai, J. *Angew. Chem. Int. Ed.* **2004**, *43*, 4338.
26. Gu, Z. Z.; Wei, H. M.; Zhang, R. Q.; Han, G. Z.; Pan, C.; Zhang, H.; Tian, X. J.; Chen, Z. M. *Appl. Phys. Lett.* **2005**, 86.
27. Singh, A.; Steely, L.; Allcock, H. R. *Langmuir* **2005**, *21*, 11604.
28. Zhou, H.; Wang, H.; Niu, H.; Gestos, A.; Wang, X.; Lin, T. *Adv. Mater.* **2012**, *24*, 2409.
29. Zhou, Q.; Xiang, H.; Fan, H.; Yang, X.; Zhao, N.; Xu, J. *J. Mater. Chem.* **2011**, *21*, 13056.
30. Martines, E.; Seunarine, K.; Morgan, H.; Gadegaard, N.; Wilkinson, C. D. W.; Riehle, M. O. *Nano Lett.* **2005**, *5*, 2097.
31. Brassard, J.-D.; Sarkar, D. K.; Perron, J. *ACS Appl. Mater. Interfaces* **2011**, *3*, 3583.
32. Kulkarni, M. M.; Yager, K. G.; Sharma, A.; Karim, A. *Macromolecules* **2012**, *45*, 4303.
33. Li, Y.; Liu, F.; Sun, J. *Chem. Commun.* **2009**, 2730.
34. Tarwal, N. L.; Khot, V. M.; Harale, N. S.; Pawar, S. A.; Pawar, S. B.; Patil, V. B.; Patil, P. S. *Surf. Coat. Technol.* **2011**, *206*, 1336.
35. Kim, E.-K.; Lee, C.-S.; Kim, S. S. *J. Colloid Interface Sci.* **2012**, *368*, 599.
36. Kim, J.-Y.; Kim, E.-K.; Kim, S. S. *J. Colloid Interface Sci.* **2013**, *392*, 376.
37. Feng, L.; Yang, Z. L.; Zhai, J.; Song, Y. L.; Lin, B. Q.; Ma, Y. M.; Yang, Z. Z.; Jiang, L.; Zhu, D. B. *Angew. Chem. Int. Ed.* **2003**, *42*, 4217.
38. Stöber, W.; Fink, A.; Bohn, E. *J. Colloid Interface Sci.* **1968**, *26*, 62.
39. Hench, L. L.; West, J. K. *Chem. Rev.* **1990**, *90*, 33.
40. Sheth, J. P.; Yilgor, E.; Erenturk, B.; Ozhalici, H.; Yilgor, I.; Wilkes, G. L. *Polymer* **2005**, *46*, 8185.
41. Jiang, P.; McFarland, M. J. *J. Am. Chem. Soc.* **2004**, *126*, 13778.
42. Xu, L.; Karunakaran, R. G.; Guo, J.; Yang, S. *ACS Appl. Mater. Interfaces* **2012**, *4*, 1118.
43. Wenzel, R. N. *Ind. Eng. Chem.* **1936**, *28*, 988.
44. Cassie, A. B. D.; Baxter, S. *Trans. Faraday Soc.* **1944**, *40*, 546.
45. Ogihara, H.; Xie, J.; Okagaki, J.; Saji, T. *Langmuir* **2012**, *28*, 4605.